Since January 2020 Elsevier has created a COVID-19 resource centre with free information in English and Mandarin on the novel coronavirus COVID-19. The COVID-19 resource centre is hosted on Elsevier Connect, the company's public news and information website.

Reproductive Toxicology 111 (2022) 135–147

Contents lists available at ScienceDirect

Reproductive Toxicology

journal homepage: www.elsevier.com/locate/reprotox

Remdesivir impairs mouse preimplantation embryo development at therapeutic concentrations

Yusuke Marikawa, Vernadeth B. Alarcon *

Institute for Biogenesis Research, Department of Anatomy, Biochemistry and Physiology, University of Hawaii John A. Burns School of Medicine, Honolulu, HI 96813, USA

ARTICLE INFO

Handling Editor: Dr. Anna Price

Keywords:
Antiviral drug
Blastocyst
COVID-19
Fertility
GS-441524
Preimplantation development
Remdesivir
Reproductive risk

ABSTRACT

Remdesivir (RDV) is the first antiviral drug to be approved by the US Food and Drug Administration for the treatment of COVID-19. While the general safety of RDV has been studied, its reproductive risk, including embryotoxicity, is largely unknown. Here, to gain insights into its embryotoxic potential, we investigated the effects of RDV on mouse preimplantation embryos cultured in vitro at the concentrations comparable to the therapeutic plasma levels. Exposure to RDV (2–8 μM) did not affect the initiation of blastocyst formation, although the maintenance of the cavity failed at 8 μM due to increased cell death. While exposure to 2–4 μM permitted the cavity maintenance, expressions of developmental regulator genes associated with the inner cell mass (ICM) lineage were significantly diminished. Adverse effects of RDV depended on the duration and timing of exposure, as treatment between the 8-cell to early blastocyst stage most sensitively affected cavity expansion, gene expressions, and cell proliferation, particularly of the ICM than the trophectoderm lineage. GS-441524, a major metabolite of RDV, did not impair blastocyst formation or cavity expansion, although it altered gene expressions in a manner differently from RDV. Additionally, RDV reduced the viability of human embryonic stem cells, which were used as a model for the human ICM lineage, more potently than GS-441524. These findings suggest that RDV is potentially embryotoxic to impair the pluripotent lineage, and will be useful for designing and interpreting further in vitro and in vivo studies on the reproductive toxicity of RDV.

1. Introduction

The coronavirus disease 2019 (COVID-19) continues to propagate and cause serious health problems worldwide, making it imperative to explore pharmaceutical treatments to ease symptoms, speed up recovery, and prevent death. The antiviral drug remdesivir (RDV) is a nucleotide analog that acts as an inhibitor of RNA-dependent RNA polymerases, thereby suppressing the proliferation of various RNA viruses, including severe acute respiratory syndrome coronavirus 2 (SARS-CoV-2), the cause of COVID-19 [30]. RDV is the first antiviral drug that was approved by the U.S. Food and Drug Administration (FDA) for the treatment of COVID-19 [15]. The efficacy of RDV against SARS-CoV-2 proliferation has been demonstrated in cultured cells, model animals, and human [16,35,46]. However, with respect to safety, RDV is implicated for the toxic effects on certain tissues and organs, although the underlying mechanisms are still unclear [1,6,13]. One of the most difficult safety assessments for many pharmaceutical drugs is reproductive toxicity, such as adverse impact on embryogenesis. This is partly because human clinical trials exclude women who are pregnant or planning to conceive. To date, information on the reproductive risk of RDV, including its embryotoxicity, is largely unknown [11,28]. While the COVID-19 pandemic persists, many women of reproductive age may require antiviral treatment while wishing to preserve their fertility. Therefore, it is crucial to obtain more information on the potential embryotoxicity of RDV.

In the present study, to gain insights into the embryotoxic property of RDV, we examined the effects of the drug on the preimplantation development of mouse embryos. The key role of preimplantation development, which takes 4–5 days after fertilization in the mouse, is to produce the blastocyst, a structure capable of implanting into the uterus [7,36,43]. The blastocyst consists of two distinct cell lineages: the trophectoderm (TE) and inner cell mass (ICM). Formation of these two lineages occurs after the 8-cell stage or embryonic day (E) 2.5 (Fig. 1). Generally, cells situated on the surface of the embryo form the TE,

* Correspondence to: Institute for Biogenesis Research, Department of Anatomy, Biochemistry and Physiology, University of Hawaii John A. Burns School of Medicine, 651 Ilalo Street, Biosciences Building 163, Honolulu, HI 96813, USA.
E-mail address: vernadet@hawaii.edu (V.B. Alarcon).

https://doi.org/10.1016/j.reprotox.2022.05.012
Received 28 February 2022; Received in revised form 5 May 2022; Accepted 18 May 2022
Available online 21 May 2022

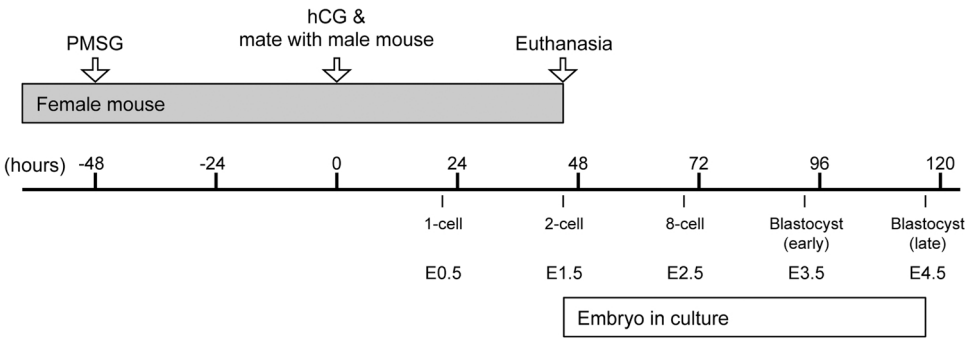

Fig. 1. A schematic diagram, depicting the superovulation and mating schedule of the mice and the embryonic stages. Hours are indicated relative to the time of the hCG injection. See Materials and methods for more details. E: embryonic day, hCG: human chorionic gonadotropin, PMSG: pregnant mare serum gonadotropin.

whereas internally located cells give rise to the ICM. The TE creates the fluid-filled cavity inside the blastocyst, the expansion of which enables the blastocyst to hatch out of the egg coat and implant. After implantation, the TE gives rise to the trophoblast tissue of the placenta. During expansion of the blastocyst cavity, the ICM subdivides into the epiblast (EPI) and primitive endoderm (PrE). The EPI is a pluripotent precursor of the fetal body, and the PrE is an extraembryonic tissue that induces the body axis in the EPI. Thus, by E4.5, the blastocyst is produced that possesses a well-expanded cavity with three tissue types (TE, EPI, and PrE). The establishment of these tissues is controlled by the interplay of specific signaling pathways and transcription factors [40,47,50,53], and interference with these molecular machineries compromises further development or survival of the embryo.

One of the advantages in using mouse preimplantation embryos for embryotoxicity studies is their robust development in vitro, i.e., completely outside of the mother. The embryos can be cultured in a chemically defined medium from fertilization [56], which efficiently develop into blastocysts, consisting of TE (with an expanded cavity), EPI, and PrE. For some genetic backgrounds of mice (e.g., crosses of B6D2F1 hybrids used in the present study), nearly all of cultured embryos can give rise to blastocysts that are competent for implantation and further postimplantation development [2,32]. Because of the in vitro nature, the effects of test drugs can be assessed at specific concentrations that are comparable to those found in the body, thus evaluating the responses of embryos to drug exposures in a pharmacologically and clinically relevant manner. Exposed embryos can be further analyzed in reference to the existing knowledge on the morphogenesis (e.g., blastocyst cavity formation) and cell differentiation (e.g., expressions of the lineage-specific genes) to identify the drug targets that are responsible for the embryotoxic actions. Accordingly, the embryotoxicity of various chemicals have been studied using mouse preimplantation embryos [3,8,17,19,64].

Here, we tested the effects of RDV and its metabolite GS-441524 (Supplemental Fig. 1), which is found in the plasma of patients receiving RDV [25,27,28,57], on cultured mouse preimplantation embryos. The drug impact was analyzed at the morphological and molecular levels to determine the concentration-effect relationships with respect to the formation of the blastocyst cavity and the establishment of the cell lineages. We also determined the developmental stage that is most sensitive to RDV exposure. Furthermore, a human pluripotent stem cell line that was originated from a human blastocyst was used as a model for the human ICM lineage to examine the effects of RDV and GS-441524.

2. Materials and methods

2.1. Test chemicals

Remdesivir (RDV) and GS-441524 (Supplemental Fig. 1) were commercially obtained from Cayman Chemicals (Ann Arbor, MI), and were dissolved in dimethyl sulfoxide (DMSO) as vehicle at 5 mM as stocks. Chemicals were further diluted in the KSOM embryo culture medium (MR-121-D; Millipore, Temecula, CA) to attain specific test concentrations. Specifically, RDV was tested at 2, 4, and 8 μM, which are comparable to the concentrations found in the plasma of patients, who received the FDA-approved therapeutic dose of the drug (C_{max} = 4.3–9.0 μM; [25,27,57]). This is to evaluate the embryotoxic effects of RDV in a clinically relevant context. GS-441524, the main metabolite of RDV, was also tested at similar concentrations, namely 4 and 8 μM, to compare with RDV. In each set of experiments, all treatment groups, including controls, contained the same final concentrations of DMSO.

2.2. Animals and collection of embryos

The protocol for animal use was approved by the Institutional Animal Care and Use Committee of the University of Hawaii, and is in accordance with the national guidelines for the care and use of animals [44]. Female and male mice of the F1 hybrid (C57BL/6 × DBA/2), i.e., B6D2F1, were purchased from Charles River Laboratories (Frederick, MD) at the age of 8 weeks old, and were cared for at an Association for Assessment and Accreditation of Laboratory Animal Care (AAALAC) accredited animal facility of the University of Hawaii. After arrival at the facility, animals were allowed to acclimate at least for one week before use. Animals were housed (6 mice or less per cage) in ventilated shoebox cages (1285 L Blue Line, Tecniplast, West Chester, PA) with hardwood chip bedding (Teklad 7115, Envigo, Indianapolis, IN) and tissue paper for enrichment. Irradiated rodent diet (2920X, Envigo) and tap water from water bottles were given ad libitum. The animal facility is kept at 21°– 23 °C with humidity level of 45–50% and light/dark cycle at 12-hour intervals. All animals were used at the age of 9–15 weeks old.

To maximize the number of embryos for experiments, superovulation was performed, according to the previously described method [5]. Briefly, females were intraperitoneally injected with 5 IU pregnant mare serum gonadotropin (Millipore) and 48 h later with 5 IU human chorionic gonadotropin (hCG; Millipore) (Fig. 1). Each female was placed in a cage overnight with a male, and the next day was examined for the presence of a copulation plug to verify successful mating. Superovulation is compatible with normal embryo development, and has been widely performed in various experimental studies to obtain many preimplantation embryos [5]. For B6D2F1 mice, nearly 100% of embryos obtained from superovulated females can give rise to blastocysts in vitro, many of which are capable of implantation and full-term development after transfer to the uteri of surrogate females [2,32]. The use of superovulation to maximize the yield of embryos per female is in line with the 3 R principle (replacement, reduction, and refinement) of ethical animal research [24,33].

At about 45 h after the hCG injection, female mice were euthanized by cervical dislocation, and the oviducts were removed. Two-cell stage embryos, which correspond to embryonic day 1.5 (E1.5) (Fig. 1), were flushed out from the isolated oviducts with the FHM medium

(Millipore). For each experiment, embryos obtained from three to four females were grouped together as a batch. Embryos were cultured in 20 μL drops of KSOM with overlying mineral oil in an incubator (37 °C with 5% CO_2 humidified air). Embryo culture was conducted in the atmospheric oxygen level (20%), which is commonly practiced and allows nearly 100% of control embryos from the B6D2F1 crossing to develop to the 8-cell stage (E2.5; 69 h after the hCG injection), the early blastocyst stage (E3.5; 93 h after the hCG injection), and the late blastocyst stage (E4.5; 117 h after the hCG injection) with a well-expanded cavity (Fig. 1).

2.3. Chemical treatment of embryos

Culture dishes with 20 μL drops of KSOM medium, containing a specific concentration of a test chemical, were overlaid with mineral oil and were equilibrated in the incubator for 2–3 h before use. To initiate treatment, embryos were transferred into a chemical-containing KSOM drop using a microcapillary glass pipet, and cultured in the incubator. After a designated duration of treatment, embryos were first photographed for morphological analysis (see Section 2.4), and then removed from drops using a microcapillary glass pipet to process for further cellular and molecular analyses (see Sections 2.5, 2.6, and 2.7).

Three different treatment protocols were employed, depending on the purpose of the experiments. For the first protocol, embryos were treated with test chemicals (RDV at 2, 4, and 8 μM; GS-441524 at 4 and 8 μM) from E2.5 (8-cell stage) up to E4.5 (late blastocyst stage) for a total of 48 h. This was to test the effects of test chemicals on the key processes of blastocyst development, namely cavity formation and cell lineage specification, which normally take place between E2.5 and E4.5. The second and third protocols were designed to evaluate how the duration and timing of exposure affect the impact of RDV. For the second protocol, embryos were treated with RDV (2, 4, and 8 μM) for a longer duration (a total of 72 h) from E1.5 (2-cell stage) to E4.5. For the third protocol, embryos were exposed to RDV (8 μM) at different intervals between E2.5 and E4.5 to examine the influence of timing-dependent exposures. Specifically, in one group, 8-cell stage embryos were cultured in RDV for 24 h followed by transfer at E3.5 into control medium for 24 h of culture up to E4.5 (designated as RDV-CON). In another group, embryos were exposed in reversed conditions, in which they were cultured in control medium for 24 h followed by transfer into RDV for 24 h (designated as CON-RDV).

2.4. Morphological analysis

Bright-field images of embryos were captured, using AxioCam MRm digital camera connected to Axiovert 200 inverted microscope with Hoffman modulation contrast optics (Carl Zeiss, Thornwood, NY). Images were converted to the JPG format, which were then opened in ImageJ program (http://rsb.info.nih.gov/ij) to analyze the size of embryos. The periphery of each embryo was manually traced using the Polygon selections tool to measure the area occupied by the embryo. The area reflects the overall size of the embryo, which dramatically increases from E2.5 to E4.5 during normal development due to the expansion of the blastocyst cavity. The expansion of the blastocyst cavity is dependent on the differentiation and structural integrity of TE [36]. Thus, the size measurement from E2.5 to E4.5 allows the evaluation of the embryo quality, particularly for TE.

2.5. Cell death assay

The extent of cell death in RDV-treated embryos was assessed using the LIVE/DEAD Cell Imaging kit (Thermo Fisher Scientific, Waltham, MA), according to the manufacturer's instruction. Fluorescence (green for LIVE and red for DEAD) and bright-field images of stained embryos were captured, using Axiovert 200 with the Colibri 2 illumination system (Carl Zeiss). To measure the area occupied by dead cells, red fluorescence images were opened in ImageJ, and converted to binary (black and white) images using the MaxEntropy method. The regions of white pixels were measured as the DEAD area for individual embryos.

2.6. Quantitative reverse transcription polymerase chain reaction (qRT-PCR)

qRT-PCR was performed to compare the transcript levels of the lineage marker genes between control and RDV- or GS-441524-treated embryos. Total RNA was extracted from each sample (20–30 embryos)

Table 1
Primer sequences for qRT-PCR analyses.

Gene name	Primer sequences (5' → 3')	Characteristics	References
Amotl2	F: TGGTTGGCTTTCCTCTGCTTTTTA R: CTGCTGGTGGGAACGAATACATTT	TE marker (E3.5)	[37]
Cdx2	F: GACTTCCTGTCCCTTCCCTCGTCT R: CCTCCCGACTTCCCTTCACCATAC	TE marker (E3.5–4.5)	[55]
Eomes	F: ATCTCCTAACACTGGCTCCCACTG R: CGTTGGTCTGTGGCACGGTTCTCT	TE marker (E4.5)	[51]
Esrrb	F: GTCCTTCCCTCCAGACTTGACTAC R: ACATCTTAAGTCATTCCAGCCACAAC	EPI marker (E4.5)	[42]
Gapdh	F: GCATGGCCTTCCGTGTTCCT R: CCCTGTTGCTGTAGCCGTATTCAT	Housekeeping	[37]
Gata3	F: CATGCTCTGTGAATCAGTCCCTGT R: AACCCTCCAGAGTACATCCACCTT	TE marker (E3.5–4.5)	[21]
Gata4	F: AGCCAAGCCCTCTTAAGTCAGACA R: CTACAGCTCTGTGGGTGATGAGGA	PrE marker (E4.5)	[26]
Nanog	F: GCTTTGGAGACAGTGAGGTGCATA R: GCTACCCTCAAACTCCTGGTCCTT	ICM/EPI marker (E3.5/E4.5)	[41]
Pdgfra	F: ATGTGGTCTGCCAACCTGTACAAA R: GTTAACGTGCCTGTGGGGAATATC	PrE marker (E4.5)	[48]
Pou5f1	F: AGGCAGGAGCACGAGTGGAAAGCA R: GGAGGGCTTCGGGCACTTCAGAAA	ICM/EPI marker (E3.5/E4.5)	[45]
Sox2	F: CACATGAAGGAGCACCCGGATTAT R: CTGGAGTGGGAGGAAGAGGTAACC	ICM/EPI marker (E3.5/E4.5)	[59]
Sox17	F: ACTGCGGAGTGAACCTCTCAGACA R: GTGTGTAACACTGCTTCTGGCCCT	PrE marker (E4.5)	[4]

Abbreviations: EPI, epiblast; ICM, inner cell mass; PrE, primitive endoderm; TE, trophectoderm.

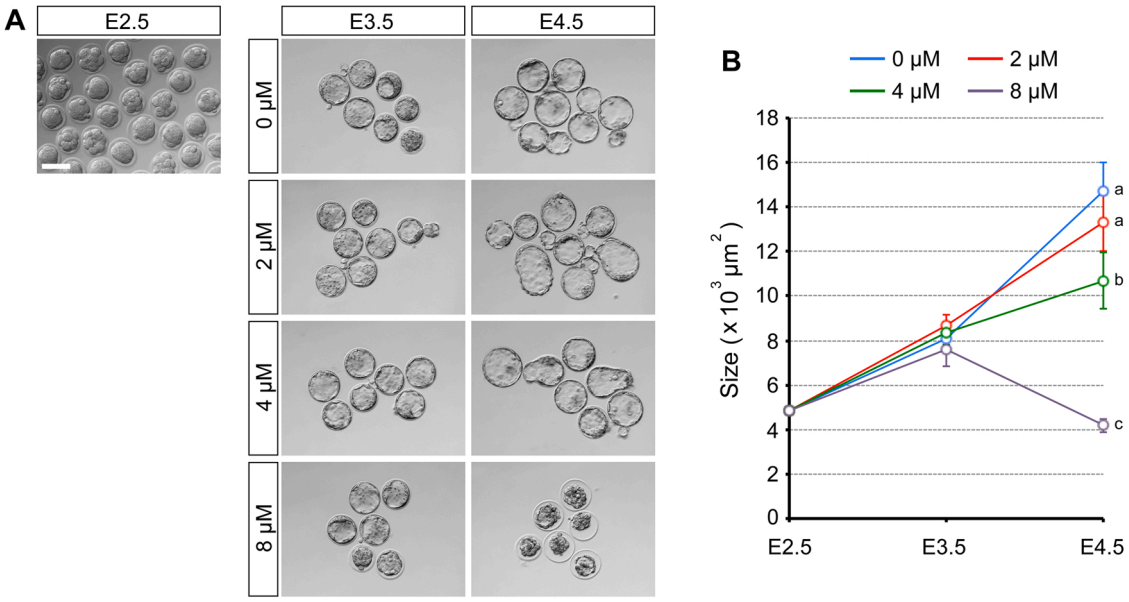

Fig. 2. Adverse effects of remdesivir (RDV) on the expansion and maintenance of the blastocyst cavity. Embryos are treated with indicated concentrations of RDV from E2.5 to E4.5. **A.** Representative images of RDV-treated embryos at E2.5 (before treatment), E3.5, and E4.5. Scale bar = 100 μm. **B.** The size of RDV-treated embryos. Different letters indicate statistically significant differences among treatments (mean ± 95% CI, n = 27 or 28 for each treatment group, one-way ANOVA followed by t-test, $p < 0.01$). No significant difference is observed among treatments at E3.5.

and processed for cDNA synthesis, according to the method described previously [37]. Quantitative PCR was performed, using the CFX96 Real-Time PCR Detection System (Bio-Rad, Hercules, CA) with SsoAdvanced Universal SYBR Green Supermix (Bio-Rad), as described previously [37]. Data files were opened in CFX Manager software (Bio-Rad), and Ct values were transferred to the Excel program for further analyses. The sequences of the primers used are listed in Table 1. The expression levels of genes were normalized with *Gapdh* as a housekeeping gene, and presented as relative expression levels, as described previously [37].

2.7. Immunofluorescence staining and confocal microscopy

Immunofluorescence staining was performed to count the number of cells that express the lineage marker proteins, namely transcription factors CDX2 (TE), SOX2 (ICM and EPI), NANOG (EPI), SOX17 (PrE), and GATA4 (PrE). Embryos were fixed, permeabilized, blocked, and incubated with antibodies, according to the method described previously [32]. Primary antibodies used were mouse anti-CDX2 (CDX2–88; Abcam, Cambridge, MA) at 1:500 dilution, rabbit anti-SOX2 (N1C3;

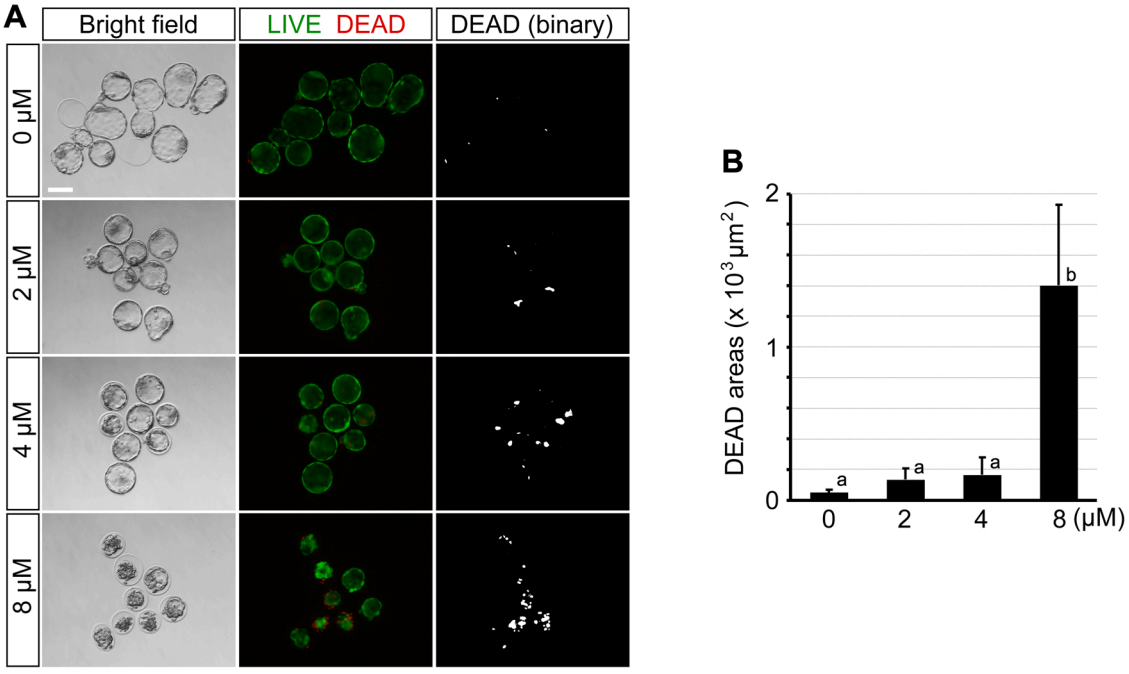

Fig. 3. Impact of remdesivir (RDV) on cell survival. Embryos are treated with indicated concentrations of RDV from E2.5 to E4.5. **A.** Representative images of RDV-treated embryos at E4.5 that are stained for live (green) and dead (red) cells by the LIVE/DEAD Cell Viability Assay. Binary images (see Materials and methods) are also shown for dead cells. Scale bar = 100 μm. **B.** The areas occupied by dead cells in RDV-treated embryos. Different letters indicate statistically significant differences among treatments (mean ± 95% CI, n = 24 or 25 for each treatment group, one-way ANOVA followed by t-test, $p < 0.01$).

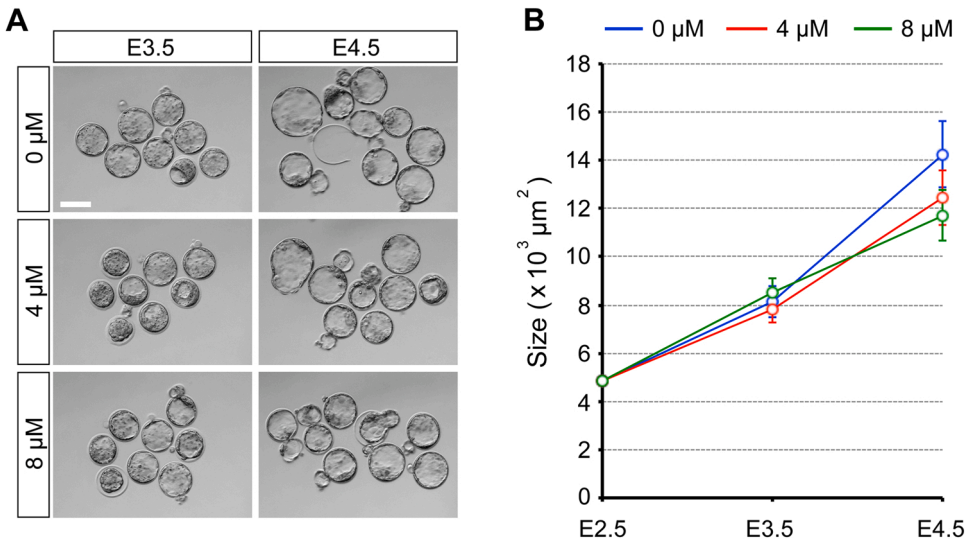

Fig. 4. Effects of GS-441524, a major metabolite of remdesivir, on the expansion and maintenance of the blastocyst cavity. Embryos are treated with indicated concentrations of GS-441524 from E2.5 to E4.5. **A.** Representative images of GS-441524-treated embryos at E3.5 and E4.5. Scale bar = 100 μm. **B.** The size of GS-441524-treated embryos. No significant difference is found at E3.5 or E4.5 among treatments (mean ± 95% CI, n = 30–32 for each treatment group).

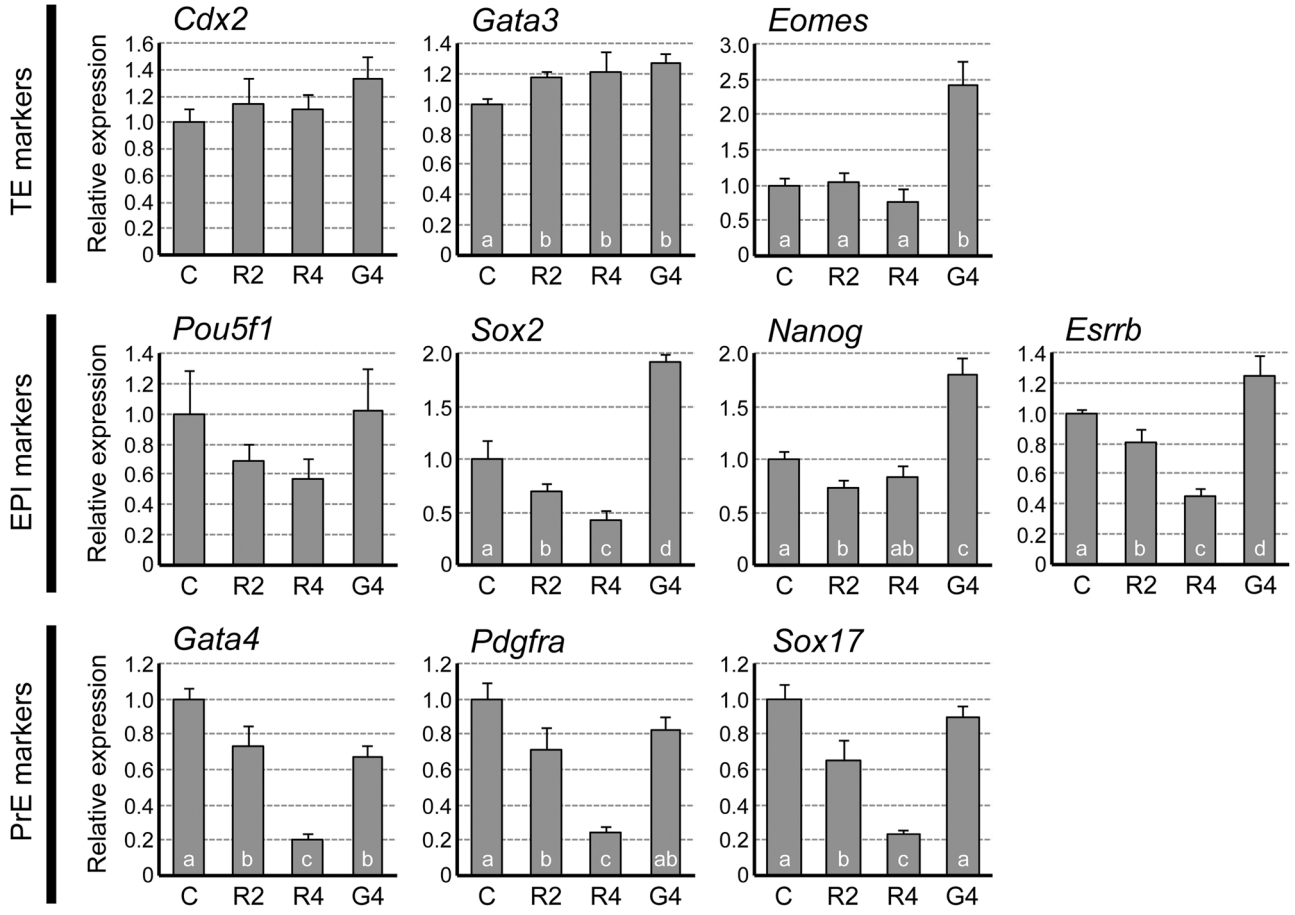

Fig. 5. Impact of remdesivir (RDV) and GS-441524 on the expression levels of the marker genes for the trophectoderm (TE), the epiblast (EPI), and the primitive endoderm (PrE) at E4.5. Embryos are treated from E2.5 to E4.5 with vehicle control (C), RDV at 2 μM (R2), RDV at 4 μM (R4), or GS-441524 at 4 μM (G4). Graphs are qRT-PCR data, showing relative expression levels of each lineage marker, normalized against housekeeping gene *Gapdh*. Different letters indicate statistically significant differences among treatments (mean ± standard deviation, n = 3 for each treatment group, one-way ANOVA followed by t-test, $p < 0.05$). No significant difference is observed for *Cdx2* and *Pou5f1*.

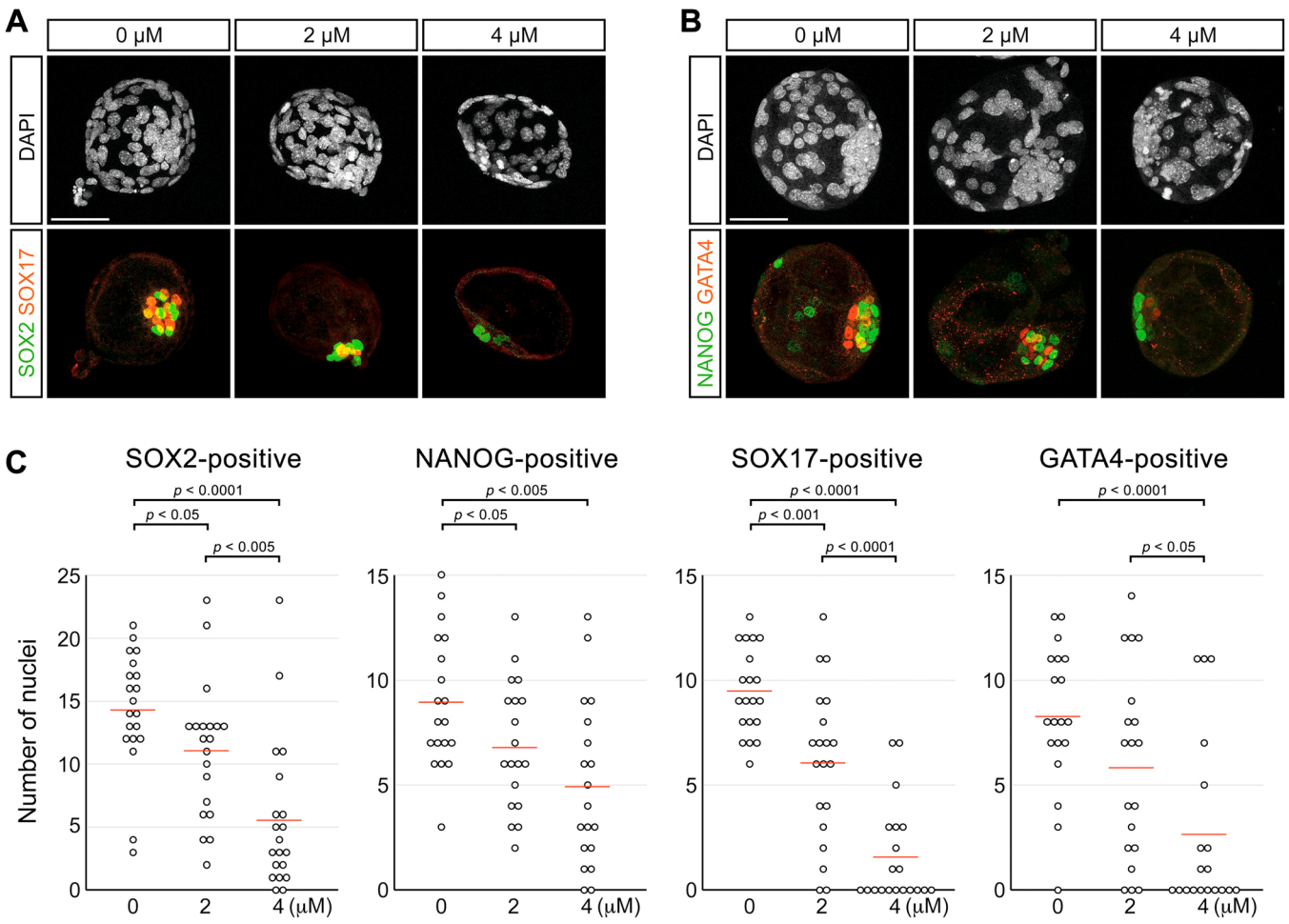

Fig. 6. Impact of remdesivir (RDV) on the epiblast (EPI) and the primitive endoderm (PrE) cells. Embryos are treated with indicated concentrations of RDV from E2.5 to E4.5, and immunohistochemically examined for SOX2 (EPI marker), NANOG (EPI marker), SOX17 (PrE marker), and GATA4 (PrE marker). **A.** Representative images of embryos that are stained for the nuclei (DAPI), SOX2 (green) and SOX17 (red). **B.** Representative images of embryos stained for the nuclei (DAPI), NANOG (green) and GATA4 (red). Scale bars = 50 μm. **C.** Numbers of nuclei that are positive for the EPI marker and PrE marker per embryo. Red lines indicate mean values (n = 19 or 20 for each treatment group). Statistically significant differences are marked with horizontal bars and p-values (t-test) between two groups.

GeneTex, Irvine, CA) at 1:200 dilution, rabbit anti-NANOG (RCAB0002P-F; Cosmo Bio USA, Carlsbad, CA) at 1:300 dilution, goat anti-SOX17 (AF1924; R&D Systems, Minneapolis, MN) at 1:100 dilution, and goat anti-GATA4 (C-20; Santa Cruz Biotechnology, Dallas, TX) at 1:50 dilution. Alexa 488- or Alexa 546-conjugated secondary antibodies were used at 1:500–1:1000 dilution (Thermo Fisher Scientific). Stained embryos were mounted in ProLong Gold medium containing 4', 6-diamidino-2-phenylindole (DAPI) to stain nuclei (Thermo Fisher Scientific), and imaged with SP8 confocal laser scanning microscope with the LAS X software (Leica Microsystems, Buffalo Grove, IL). Serial optical sections of entire embryos were obtained at 2 μm intervals under a 60 × oil objective lens. Image files were converted to a series of TIFF files, which were opened with the ImageJ program. For each embryo, the total number of cells based on DAPI staining, and the number of nuclei positive for a lineage-marker were counted by examining the entire series of optical sections.

2.8. Human embryonic stem cell viability assay

H9 line (WA09, National Institutes of Health registration number 0062) of human embryonic stem cells was obtained from WiCell Research Institute (Madison, WI). Cells were maintained in the mTeSR culture medium (Stemcell Technologies, Vancouver, BC, Canada) with iMatrix-511 (Takara Bio, Mountain View, CA), as previously described [38]. The impact of RDV and GS-441524 on cell proliferation under the maintenance condition was evaluated using the CellTiter-Glo Luminescent Cell Viability Assay system, which measures the amount of ATP as a quantitative proxy for the number of metabolically active cells (Promega, Madison, WI). H9 cells were seeded in 96-well plates at a density of 500 cells/well with 50 μL of mTeSR. After one day of culture, 50 μL of mTeSR containing a test chemical (2 times of the desired concentration) was added to start a treatment. The same final concentrations (0.16%) of DMSO were included in all treatment groups. After 2 days of treatments, cells were lysed and incubated for 15 min in 80 μL of an equal volume mixture of the CellTiter-Glo Reagent and phosphate-buffered saline. Luminescence intensity of lysate was measured as relative light unit using Gene Light 55 Luminometer (Microtech, Chiba, Japan). Cell seeding density was optimized through a series of pilot experiments to confirm that cell numbers at the end of culture were proportionate to intensities of luminescence.

2.9. Data analyses and statistics

All experiments were conducted at least three times, using different batches of pooled embryos or cell collections as biological replicates, and compiled data were presented as mean ± standard deviation. When three or more treatment groups were compared, the one-way analysis of variance (ANOVA) was used to determine whether there were any significant differences among their means, which was then followed by post-hoc two-sample t-test to compare between two specific groups.

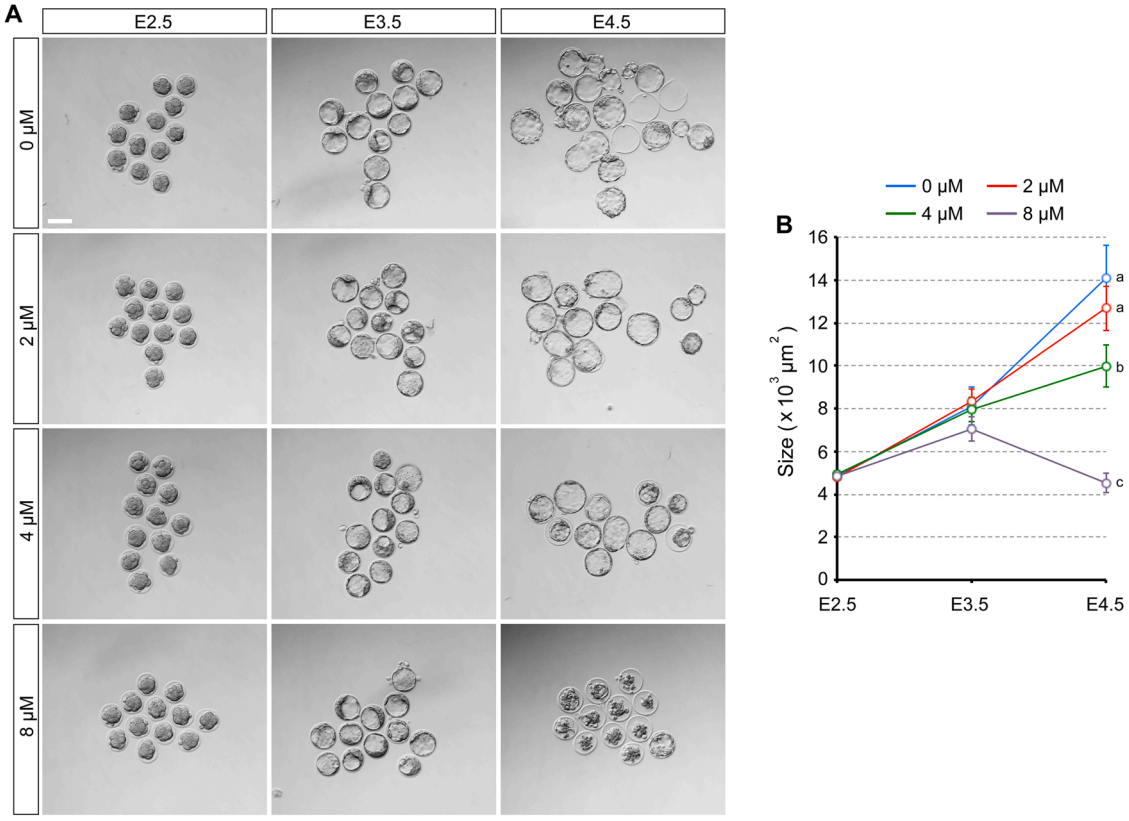

Fig. 7. Impact of early exposure to remdesivir (RDV) on the expansion and maintenance of the blastocyst cavity. Embryos are treated with indicated concentrations of RDV from E1.5 to E4.5. **A.** Representative images of RDV-treated embryos at E2.5, E3.5, and E4.5. Scale bar = 100 μm. **B.** The size of RDV-treated embryos. Different letters indicate statistically significant differences among treatments (mean ± 95% CI, n = 36–40 for each treatment group, one-way ANOVA followed by t-test, $p < 0.01$). No significant difference is observed among treatments at E3.5.

3. Results

3.1. Remdesivir, but not its metabolite GS-441524, impairs the expansion and maintenance of the blastocyst cavity

When embryos were treated with RDV (2, 4, and 8 μM) from E2.5 (8-cell stage), all treatment groups had formed a blastocyst cavity by E3.5 (Fig. 2A). Their sizes and gross morphology were indistinguishable from the control embryos (0 μM; vehicle only) (Fig. 2B). By E4.5, embryos exposed to 2 μM RDV further expanded the cavity similarly to the control, and those exposed to 4 μM RDV also expanded but less robustly than the control (Fig. 2B). By contrast, embryos exposed to 8 μM RDV had collapsed their cavity (Fig. 2A), resulting in a significantly decreased size (Fig. 2B). These results suggest that RDV treatment does not affect the initial blastocyst formation up to E3.5, but impairs the expansion (at 4 μM) or the maintenance (at 8 μM) of the cavity by E4.5.

The decrease in size upon RDV exposure implicates the possibility that the blastocysts are undergoing cell death. To test this possibility, RDV-treated E4.5 embryos were stained for live and dead cells. Embryos exposed to the lower concentrations (2 and 4 μM) had some patches of dead cells (Fig. 3A), but the areas occupied by them were not significantly larger than the control (Fig. 3B). By contrast, treatment with 8 μM RDV caused a dramatic increase in areas containing dead cells (Fig. 3A, B). This suggests that exposure to the high concentration of RDV leads to cell death, causing a collapse of the blastocyst cavity by E4.5.

By contrast, embryos treated with GS-441524 (4 or 8 μM) from E2.5 developed into expanded blastocysts by E4.5 in a manner comparable to the control in terms of size and gross morphology (Fig. 4). Thus, in spite of the similarity to RDV in chemical structure (Supplemental Fig. 1), GS-441524 did not impair the blastocyst cavity formation or maintenance at the concentrations equivalent to those tested for RDV.

3.2. Remdesivir diminishes the gene expressions associated with the inner cell mass lineage

To evaluate the state of RDV-exposed blastocysts at the molecular level, the gene expression profiles of key cell lineage markers were examined at E4.5. The transcript levels of TE markers *Cdx2* and *Eomes* were unchanged, while *Gata3* was increased by about 20% by RDV exposure (Fig. 5). By contrast, the expressions of the epiblast (EPI) markers were mostly reduced by RDV exposure. Specifically, the transcript levels of *Sox2* and *Esrrb* were progressively decreased in a concentration-dependent manner, with about 55% reduction at 4 μM. *Pou5f1* expression also appeared to be diminished progressively, although not statistically significant. *Nanog* expression was significantly decreased by RDV at 2 μM, but not at 4 μM. The expressions of the primitive endoderm (PrE) markers, *Gata4*, *Pdgfra*, and *Sox17*, were all progressively down-regulated by RDV exposure, with 75–80% reduction at 4 μM. These results suggest that RDV mainly diminishes the gene expressions associated with the ICM lineage (i.e., EPI and PrE) but not the TE lineage.

For comparison, the gene expression profiles were also examined for the blastocysts that were exposed to GS-441524 at 4 μM. GS-441524 altered the expressions of some of the cell lineage markers, although the patterns of alterations differed from RDV (Fig. 5). Most notably, GS-441524 significantly increased the levels of the EPI markers, *Sox2*, *Nanog*, and *Esrrb*, which was opposite to the effects of RDV. Thus, the impacts of RDV and GS-441524 on preimplantation embryos were different from each other at the morphological and molecular levels.

The reduction in the EPI and PrE marker transcripts by RDV exposure was accompanied by a decrease in the cell number of these tissues. Immunofluorescence staining showed that the numbers of nuclei positive for EPI marker proteins (SOX2 and NANOG) and those positive for

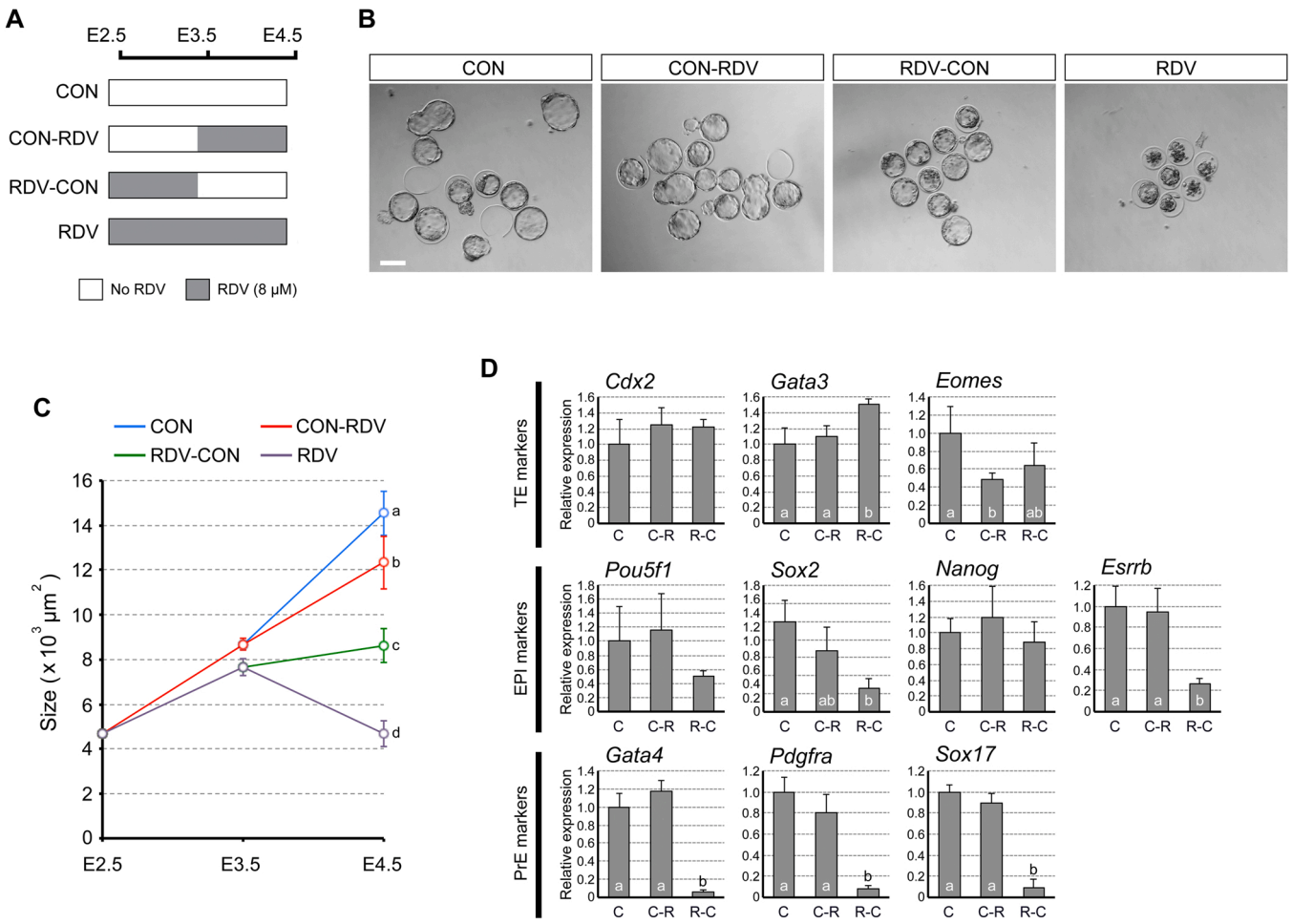

Fig. 8. Duration- and timing-dependent impact of remdesivir (RDV) exposure on the blastocyst morphology and the gene expression profiles. **A.** A diagram depicting the RDV treatment regimen. **B.** Representative images of treated embryos at E4.5. Scale bar = 100 μm. **C.** The size of treated embryos. Different letters indicate statistically significant differences among treatments (mean ± 95% CI, n = 30–54 for each treatment group, one-way ANOVA followed by t-test, $p < 0.01$). **D.** The expression levels of the markers for the trophectoderm (TE), the epiblast (EPI), and the primitive endoderm (PrE) at E4.5. Graphs are qRT-PCR data, showing relative expression levels of each lineage marker, normalized against housekeeping gene *Gapdh*. C, C-R, and R-C correspond to the treatment groups CON, CON-RDV, and RDV-CON, depicted in **A**, respectively. The RDV group is not analyzed due to extensive cell death. Different letters indicate statistically significant differences among treatments (mean ± standard deviation, n = 3 for each treatment group, one-way ANOVA followed by t-test, $p < 0.05$). No significant difference is observed for *Cdx2, Pou5f1*, and *Nanog*.

PrE marker proteins (SOX17 and GATA4) were significantly lower in RDV-treated E4.5 blastocysts (Fig. 6). Thus, in spite of the normal appearance in the gross morphology, the formation of EPI and PrE was diminished in blastocysts treated with RDV even at 2 μM.

3.3. Adverse effects of remdesivir depend on the duration and timing of exposure

To determine whether preimplantation development is more severely impaired when RDV exposure starts before the 8-cell stage, embryos were treated from E1.5 (2-cell stage). All treatment groups (0, 2, 4, and 8 μM) progressed to the 8-cell stage by E2.5, and developed into blastocysts by E3.5 (Fig. 7A). By E4.5, embryos treated with 2 μM RDV further expanded the cavity in a manner comparable to the control (0 μM), whereas those treated with 4 μM expanded less robustly (Fig. 7B). The cavity collapsed in most of the blastocysts exposed to 8 μM RDV. Overall, the concentration-effect relationship was essentially indistinguishable from the RDV treatment started from E2.5 (Fig. 2), indicating that earlier treatment from E1.5 did not significantly exacerbate the effects of RDV on the cavity maintenance. This suggests that embryos are impaired by RDV when exposure occurs after the 8-cell stage.

To further examine whether the effects of RDV depend on the duration and timing of exposure, embryos were treated with RDV (8 μM) at different intervals between E2.5 and E4.5, as depicted in Fig. 8A. We observed that CON-RDV embryos formed expanded blastocysts that were slightly smaller than CON embryos (Fig. 8B,C). By contrast, RDV-CON embryos formed blastocysts that were much smaller in size relative to CON and CON-RDV blastocysts. However, RDV-CON embryos did not collapse the cavity, unlike RDV embryos (Fig. 8B,C). Thus, the blastocyst cavity expansion was more sensitively affected by the early exposure to RDV (E2.5-E3.5) than the late exposure (E3.5-E4.5), although it was most impaired with continuous exposure (E2.5-E4.5).

We then compared the expression profiles of cell lineage markers among the E4.5 blastocysts of CON, CON-RDV, and RDV-CON groups. In CON-RDV blastocysts, the effect of RDV was mild such that only 1 out of the 10 genes examined was altered, namely *Eomes* (TE; decreased) (Fig. 8D). By contrast, in RDV-CON blastocysts, the impact was much more dramatic, as expressions of 6 out of the 10 genes were altered, namely *Gata3* (TE; increased), *Sox2* and *Esrrb* (EPI; decreased), and *Gata4*, *Pdgfra*, and *Sox17* (PrE; decreased) (Fig. 8D). Notably, all of the PrE markers were reduced by greater than 80%. Altogether, these results suggest that RDV impairs the blastocyst morphology (cavity expansion) and gene expressions (the ICM lineage) most severely when exposure occurs between E2.5 and E3.5.

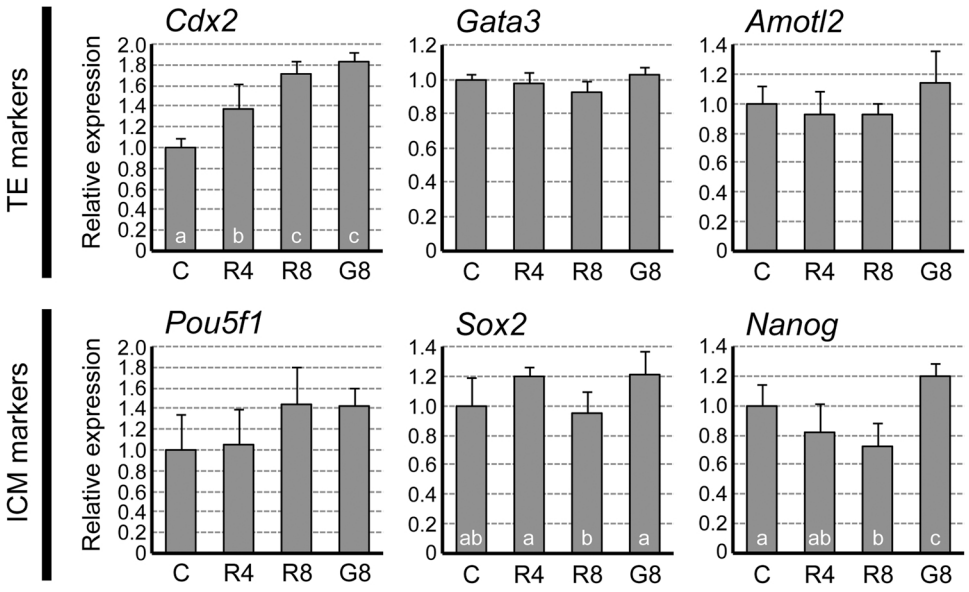

Fig. 9. Impact of remdesivir (RDV) on the trophectoderm (TE) and the inner cell mass (ICM) at E3.5. Embryos are treated from E2.5 to E3.5 with vehicle control (C), RDV at 4 μM (R4), RDV at 8 μM (R8), or GS-441524 at 8 μM (G8). Graphs are qRT-PCR data, showing relative expression levels of TE and ICM markers, normalized against housekeeping gene *Gapdh*. Different letters indicate statistically significant differences among treatments (mean ± standard deviation, n = 4 for each treatment group, one-way ANOVA followed by t-test, $p < 0.05$). No significant difference is observed for *Gata3, Amotl2,* and *Pou5f1*.

3.4. Remdesivir diminishes the proliferation of the inner cell mass lineage

Although exposure during E2.5 to E3.5 resulted in the most severe outcome by E4.5 (Fig. 8), RDV-exposed embryos appeared morphologically normal at E3.5 (Fig. 2). To assess whether adverse effects already exist at E3.5 at the molecular levels, early lineage markers for ICM and TE were compared between control and RDV-exposed embryos. For TE markers, the expression of *Cdx2* was up-regulated by RDV (4 and 8 μM), whereas *Gata3* and *Amotl2* were unaffected (Fig. 9). For ICM markers, the expression of *Nanog* was down-regulated by RDV (8 μM), while *Pou5f1* and *Sox2* were not significantly altered compared to the control (Fig. 9). By comparison, exposure to GS-441524 (8 μM) led to increases in both *Cdx2* and *Nanog*.

The total number of cells per embryo was progressively reduced by RDV treatment in a concentration-dependent manner (Fig. 10A,B). The numbers of CDX2-positive (TE) and SOX2-positive (ICM) nuclei were also lower in RDV-treated blastocysts. However, when the ratio of SOX2-positive to CDX2-positive cell numbers was analyzed for individual embryos (SOX2/CDX2 ratio), the mean ratio decreased in RDV-treated blastocysts in a dose-dependent manner (Fig. 10C). This suggests that RDV diminishes the overall cell proliferation during E2.5 to E3.5, but more severely for the ICM than TE lineage.

3.5. Remdesivir reduces the viability of human embryonic stem cells at the therapeutic concentrations

The results above on mouse embryos raised the possibility that RDV may also impair human preimplantation development. However, testing the effects of RDV on actual human embryos is practically and ethically challenging. Here, to gain insights into the potential impact of RDV on human embryos, we used human embryonic stem cells (hESCs) as a model for the human ICM lineage. RDV exposure (0.5–8 μM) significantly decreased the viability of hESCs in a concentration-dependent manner (Fig. 11). Namely, 0.5 μM RDV decreased the cell number to about 70% of the control level, whereas 4 and 8 μM RDV reduced it down to less than 10% (Fig. 11). On the other hand, GS-441524 had no effect on cell viability at 0.5–4 μM, whereas cell number decreased to 80% of the control level at 8 μM (Fig. 11). These results suggest that RDV, but not GS-441524, severely impairs the proliferation and/or survival of human cells of the ICM lineage at the concentrations found in the plasma.

4. Discussion

Here, we exploited the in vitro development of mouse preimplantation embryos to assess the adverse impact of RDV, which revealed that embryo development was severely impaired at the clinically relevant concentrations (2–8 μM). As the COVID-19 pandemic continues, pharmaceutical interventions are critical to minimize mortality and morbidity for many people, including women of reproductive age. Thus, further investigations are crucial to determine the embryotoxicity of RDV, particularly in vivo. Experimentations using pregnant animals, such as rats and rabbits, are regarded as the gold standard in the predictive assessment of the reproductive toxicity of pharmaceutical drugs [52]. However, many drugs are metabolized differently in the body between human and animals, which can significantly influence the levels of embryonic exposures. For example, in the mouse, RDV is quickly metabolized to GS-441524, so the plasma C_{max} of RDV (<1 μM) is considerably lower than that of GS-441524 (35.8 μM) [23]. This is in stark contrast to the human situation, where RDV is metabolized more slowly, so its plasma C_{max} (4.3–9.0 μM) is higher than GS-441524 (0.48–0.52 μM) [25,57]. To achieve the RDV levels that are equivalent to human in the mouse body, markedly higher doses of RDV would be required, which results in extremely high plasma concentrations of GS-441524. This may make it difficult, or impossible, to recreate in animals the exposure levels of RDV and its metabolites that are comparable to human. Therefore, in vitro studies, as in the present study, can provide opportunities to examine the concentration-effect relationship of RDV as well as its metabolites in a clinically relevant manner.

In the present study, the effects of RDV were tested at the human plasma concentrations, assuming that preimplantation embryos are potentially exposed to similar levels in vivo. It is currently unknown whether the concentrations of RDV in the fallopian tubes, where the preimplantation development normally takes place, are close to the levels in the plasma. Thus, additional pharmacokinetic information, namely on the drug distribution in the human reproductive tract, may be necessary to interpret the results of the present study. Nonetheless, it has been shown in the mouse that the RDV concentrations are 2.2- to 20.4-times higher in various organs than in the plasma, including the brain, heart, lung, kidney, liver, intestine, and testis [58]. If this is also the case for the fallopian tubes, preimplantation embryos may be exposed to higher concentrations of RDV than the plasma levels.

To our knowledge, the present study is the first to demonstrate the adverse impact of RDV on developing embryos, causing the collapse of

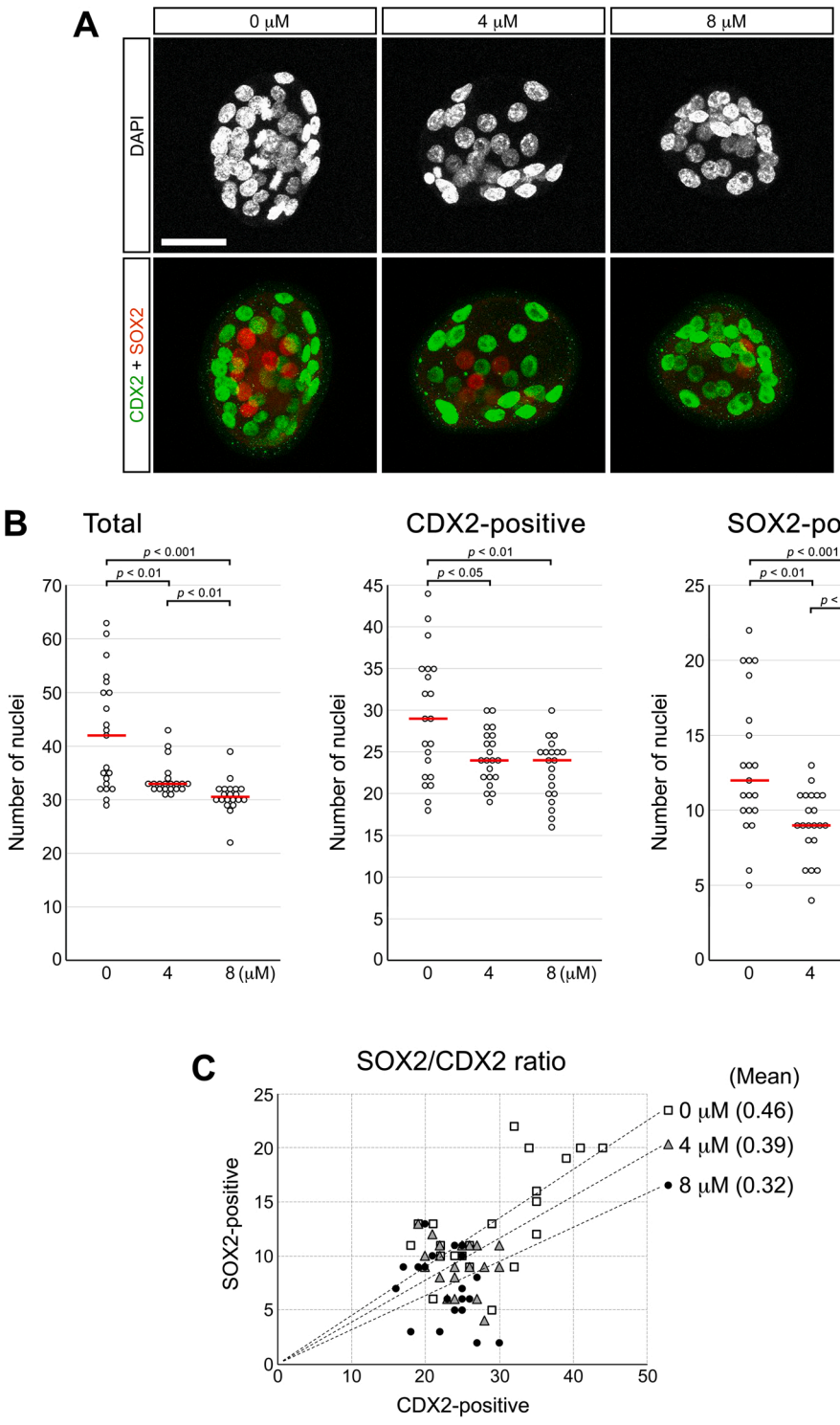

Fig. 10. Effects of remdesivir (RDV) on the trophectoderm (TE) and the inner cell mass (ICM) at E3.5. Embryos are treated with RDV from E2.5 to E3.5, and immunohistochemically examined for CDX2 and SOX2 proteins, which are markers for TE and ICM, respectively. **A.** Representative images of RDV-treated embryos that are stained for the nuclei (DAPI), CDX2 (green), and SOX2 (red). Scale bar = 50 μm. **B.** Numbers of total nuclei, and those of CDX2-positive and SOX2-positive nuclei. Red lines indicate mean values (n = 19 or 20 for each treatment group). Statistically significant differences are marked with horizontal bars and p-values (t-test) between two groups. **C.** Distribution of SOX2-positive and CDX2-positive nuclear numbers for individual embryos. Linear trend lines representing the means of the SOX2/CDX2 ratios are superimposed for each treatment group (n = 19 or 20).

the blastocyst cavity at a high concentration (8 μM) and diminishing the formation of the ICM lineage at lower concentrations (2 and 4 μM). It is unclear whether these embryotoxic effects are related to the cytotoxicity of RDV that is observed in primary and immortalized cells of various tissues [1,9,31,60]. The cytotoxicity of RDV on these cells are manifested as a significant decrease in the number of metabolically active cells (due to reduced proliferation or increased death) or impaired activities of mitochondria. Interestingly, the sensitivity to RDV varies considerably among different cell types. For example, in the case of primary cells, the 50% cytotoxic concentration (CC_{50}) is 14.8 μM for peripheral blood mononuclear cells, and 2.5 μM for hepatocytes. In the case of immortalized cell lines, CC_{50} is 8.9 μM for the PC-3 prostate adenocarcinoma cell line, and 1.7 μM for the MT-4 T-cell line [60]. The molecular nature of such cell type-specific differences in the sensitivity is unclear, although it is speculated that differences in the drug permeability and the efficacy of intracellular metabolism may play a role. Here, we showed that the ICM lineage is more sensitively affected by RDV than the TE lineage. There are significant differences in the gene expression profiles between the presumptive ICM and TE cells even at the 16-cell stage [12,18,49,61]. The pattern of the energy metabolism is

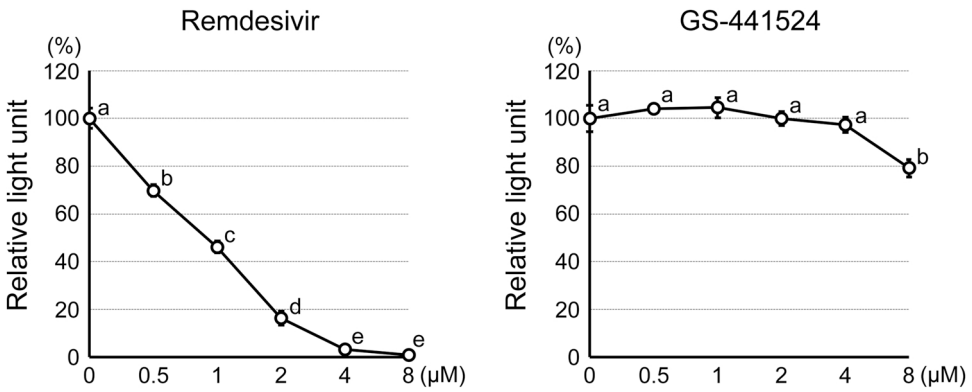

Fig. 11. Impact of remdesivir and GS-441524 on the proliferation and viability of human embryonic stem cells. Graphs show the relative light unit of the CellTiter-Glo Luminescent Assay as a proxy for the relative number of metabolically active cells after 2 days of treatment. Different letters indicate statistically significant differences among treatments (mean ± standard deviation, n = 3 for each treatment group, one-way ANOVA followed by t-test, $p < 0.01$).

also different between TE and ICM. Namely, the anaerobic glycolysis is more active in ICM, whereas the oxidative phosphorylation is more active in TE [20,22]. These differences may influence the uptake and intracellular metabolism of RDV.

The present study also demonstrated the differences in the embryotoxic effects between RDV and its main metabolite GS-441524. In various types of cells, both RDV and GS-441524 are converted to the triphosphate form (GS-443902), which acts as an inhibitor of viral RNA-dependent RNA polymerases [10,30,34]. It is unclear whether RDV and GS-441524 are converted to GS-443902 in the preimplantation embryo. Interestingly, the enzymes responsible for the conversion of RDV into GS-443902 appear to be robustly expressed in mouse E3.5 early blastocysts, namely, *Ctsa* (encoding cathepsin A), *Hint1* (encoding histidine triad nucleotide-binding protein 1), and *Ak2/4/6*, (encoding adenylate kinases), according to our previous RNA-seq study [39]. By contrast, the enzyme required for the conversion of GS-441524 into GS-443902, specifically *Adk* (encoding adenosine kinase), is only marginally expressed in E3.5 embryos [39]. This suggests that RDV, but not GS-441524, may be converted into the active triphosphate form in embryos to exert the adverse effects, which may account for the potent and severe embryotoxic effects of RDV. Note that the expression levels of several genes were altered by GS-441524 in a manner different from RDV (Figs. 5 and 9): the epiblast markers (*Sox2*, *Nanog*, and *Esrrb*) were up-regulated by GS-441524, whereas they were down-regulated by RDV. This raises the possibility that the molecular actions of GS-441524 and RDV on preimplantation development are significantly different from each other, and may not be mediated by their conversion to the triphosphate form.

While we used mouse embryos to evaluate the embryotoxicity of RDV in the present study, they may respond to RDV differently from human embryos. Experimentations using human embryos would be ideal to assess human embryotoxicity. However, it is highly challenging to conduct extensive studies with actual human embryos for ethical and practical reasons. Recent studies have shown that human pluripotent stem cells can be used to create “blastoids”, which resemble blastocysts at the morphological and molecular levels [14,29,54,62,63]. Human blastoids may be explored as in vitro alternatives of human preimplantation embryos to evaluate the adverse effects of RDV, although the validity of using blastoids for toxicity assessment needs to be investigated first in reference to various known embryotoxic chemicals.

Funding

This work was supported by the National Institutes of Health (grant numbers HD088839, HD102502, HD101735, and GM131944).

Author contribution statement

Y.M. and V.B.A. designed the research study, performed the research, analyzed the data, and wrote the paper.

Declaration of Competing Interest

The authors declare the following financial interests/personal relationships which may be considered as potential competing interests: Vernadeth Alarcon reports financial support was provided by National Institutes of Health. Yusuke Marikawa reports financial support was provided by National Institutes of Health.

Data Availability

Data will be made available on request.

Acknowledgements

We are grateful to Dr. Matthew Pitts of the University of Hawaii Health Sciences Microscopy and Imaging Core for his assistance with the confocal microscopy operation. We also thank the Animal and Veterinary Service staff of the University of Hawaii for providing care for our mice.

Appendix A. Supporting information

Supplementary data associated with this article can be found in the online version at doi:10.1016/j.reprotox.2022.05.012.

References

[1] E. Akinci, M. Cha, L. Lin, G. Yeo, M.C. Hamilton, C.J. Donahue, H.C. Bermudez-Cabrera, L.C. Zanetti, M. Chen, S.A. Barkal, B. Khowpinitchai, N. Chu, M. Velimirovic, R. Jodhani, J.D. Fife, M. Sovrovic, P.A. Cole, R.A. Davey, C. A. Cassa, R.I. Sherwood, Elucidation of remdesivir cytotoxicity pathways through genome-wide CRISPR-Cas9 screening and transcriptomics, bioRxiv (2020), https://doi.org/10.1101/2020.08.27.270819. PMID: 32869031; PMCID: PMC7457617.

[2] V.B. Alarcón, Y. Marikawa, Deviation of the blastocyst axis from the first cleavage plane does not affect the quality of mouse postimplantation development, Biol. Reprod. 69 (4) (2003) 1208–1212, https://doi.org/10.1095/biolreprod.103.018283. Epub 2003 May 28.

[3] V.B. Alarcon, Y. Marikawa, Statins inhibit blastocyst formation by preventing geranylgeranylation, Mol. Hum. Reprod. 22 (5) (2016) 350–363, https://doi.org/10.1093/molehr/gaw011. Epub 2016 Feb 7.PMID: 26908642; PMCID: PMC4847613.

[4] J. Artus, A. Piliszek, A.K. Hadjantonakis, The primitive endoderm lineage of the mouse blastocyst: sequential transcription factor activation and regulation of differentiation by Sox17, Dev. Biol. 350 (2) (2011) 393–404, https://doi.org/10.1016/j.ydbio.2010.12.007. Epub 2010 Dec 10.PMID: 21146513; PMCID: PMC3461954.

[5] R. Behringer, M. Gertsenstein, K.V. Nagy, A. Nagy, Manipulating the mouse embryo: a laboratory manual. Cold Spring Harbor Laboratory Press, fourth ed., Cold Spring Harbor, New York, 2014, pp. 105–106.
[6] J.A. Bjork, K.B. Wallace, Remdesivir; molecular and functional measures of mitochondrial safety, Toxicol. Appl. Pharmacol. 433 (2021), 115783, https://doi.org/10.1016/j.taap.2021.115783. Epub 2021 Nov 2.PMID: 34740633; PMCID: PMC8562045.
[7] C. Chazaud, Y. Yamanaka, Lineage specification in the mouse preimplantation embryo, Development 143 (7) (2016) 1063–1074, https://doi.org/10.1242/dev.128314.
[8] Y. Chen, S. Kong, X. Tang, Y. Fu, B. Wang, S. Zhang, H. Wang, Preimplantation mouse embryo is a target for opioid ligand-receptor signaling, Biol. Reprod. 91 (1) (2014) 4, https://doi.org/10.1095/biolreprod.114.118083. Epub 2014 May 22. PMID: 24855103.
[9] S.W. Choi, J.S. Shin, S.J. Park, E. Jung, Y.G. Park, J. Lee, S.J. Kim, H.J. Park, J. H. Lee, S.M. Park, S.H. Moon, K. Ban, Y.Y. Go, Antiviral activity and safety of remdesivir against SARS-CoV-2 infection in human pluripotent stem cell-derived cardiomyocytes, Antivir. Res. 184 (2020), 104955, https://doi.org/10.1016/j.antiviral.2020.104955. Epub 2020 Oct 19. PMID: 33091434; PMCID: PMC7571425.
[10] R.T. Eastman, J.S. Roth, K.R. Brimacombe, A. Simeonov, M. Shen, S. Patnaik, M. D. Hall, Remdesivir: A review of its discovery and development leading to emergency use authorization for treatment of COVID-19, ACS Cent. Sci. (2020) 672–683, https://doi.org/10.1021/acscentsci.0c00489.
[11] EMA (European Medicines Agency). Summary on compassionate use, Remdesivir Gilead. 2020 ⟨https://www.ema.europa.eu/en/documents/other/summary-compassionate-use-remdesivir-gilead_en.pdf⟩. (Accessed on 2/25/2022).
[12] X. Fan, D. Tang, Y. Liao, P. Li, Y. Zhang, M. Wang, F. Liang, X. Wang, Y. Gao, L. Wen, D. Wang, Y. Wang, F. Tang, Single-cell RNA-seq analysis of mouse preimplantation embryos by third-generation sequencing, PLoS Biol. 18 (12) (2020), e3001017, https://doi.org/10.1371/journal.pbio.3001017. PMID: 33378329; PMCID: PMC7773192.
[13] Q. Fan, B. Zhang, J. Ma, S. Zhang, Safety profile of the antiviral drug remdesivir, Update Biomed. Pharm. 130 (2020), 110532, https://doi.org/10.1016/j.biopha.2020.110532. Epub 2020 Jul 22. PMID: 32707440; PMCID: PMC7373689.
[14] Y. Fan, Z. Min, S. Alsolami, Z. Ma, E. Zhang, W. Chen, K. Zhong, W. Pei, X. Kang, P. Zhang, Y. Wang, Y. Zhang, L. Zhan, H. Zhu, C. An, R. Li, J. Qiao, T. Tan, M. Li, Y. Yu, Generation of human blastocyst-like structures from pluripotent stem cells, Cell Discov. 7 (1) (2021) 81, https://doi.org/10.1038/s41421-021-00316-8. PMID: 34489415; PMCID: PMC8421367.
[15] FDA (U.S. Food and Drug Administration). FDA's approval of Veklury (remdesivir) for the treatment of COVID-19 — the science of safety and effectiveness. 2022 ⟨https://www.fda.gov/drugs/news-events-human-drugs/fdas-approval-veklury-remdesivir-treatment-covid-19-science-safety-and-effectiveness⟩. (Accessed on 2/21/2022).
[16] J.D. Goldman, D.C.B. Lye, D.S. Hui, K.M. Marks, R. Bruno, R. Montejano, C. D. Spinner, M. Galli, M.Y. Ahn, R.G. Nahass, Y.S. Chen, D. SenGupta, R.H. Hyland, A.O. Osinusi, H. Cao, C. Blair, X. Wei, A. Gaggar, D.M. Brainard, W.J. Towner, J. Muñoz, K.M. Mullane, F.M. Marty, K.T. Tashima, G. Diaz, A. Subramanian, GS-US-540-5773 Investigators. Remdesivir for 5 or 10 Days in Patients with Severe Covid-19, New Engl. J. Med. 383 (19) (2020) 1827–1837, https://doi.org/10.1056/NEJMoa2015301. Epub 2020 May 27. PMID: 32459919; PMCID: PMC7377062.
[17] A.R. Greenlee, T.M. Ellis, R.L. Berg, Low-dose agrochemicals and lawn-care pesticides induce developmental toxicity in murine preimplantation embryos, Environ. Health Perspect. 112 (6) (2004) 703–709, https://doi.org/10.1289/ehp.6774. PMID: 15121514; PMCID: PMC1241965.
[18] G. Guo, M. Huss, G.Q. Tong, C. Wang, L. Li Sun, N.D. Clarke, P. Robson, Resolution of cell fate decisions revealed by single-cell gene expression analysis from zygote to blastocyst, Apr 20, Dev. Cell 18 (4) (2010) 675–685, https://doi.org/10.1016/j.devcel.2010.02.012.
[19] M.A. Hausburg, G.K. Dekrey, J.J. Salmen, M.R. Palic, C.S. Gardiner, Effects of paraquat on development of preimplantation embryos in vivo and in vitro (Jul-Aug), Reprod. Toxicol. 20 (2) (2005) 239–246, https://doi.org/10.1016/j.reprotox.2005.03.006.
[20] L.C. Hewitson, H.J. Leese, Energy metabolism of the trophectoderm and inner cell mass of the mouse blastocyst, Nov 1, J. Exp. Zool. 267 (3) (1993) 337–343, https://doi.org/10.1002/jez.1402670310.
[21] P. Home, S. Ray, D. Dutta, I. Bronshteyn, M. Larson, S. Paul, GATA3 is selectively expressed in the trophectoderm of peri-implantation embryo and directly regulates Cdx2 gene expression, J. Biol. Chem. 284 (42) (2009) 28729–28737, https://doi.org/10.1074/jbc.M109.016840. Epub 2009 Aug 21. PMID: 19700764; PMCID: PMC2781418.
[22] F.D. Houghton, Energy metabolism of the inner cell mass and trophectoderm of the mouse blastocyst (Feb), Differentiation 74 (1) (2006) 11–18, https://doi.org/10.1111/j.1432-0436.2006.00052.x.
[23] W.J. Hu, L. Chang, Y. Yang, X. Wang, Y.C. Xie, J.S. Shen, B. Tan, J. Liu, Pharmacokinetics and tissue distribution of remdesivir and its metabolites nucleotide monophosphate, nucleotide triphosphate, and nucleoside in mice, Acta Pharm. Sin. 42 (7) (2021) 1195–1200, https://doi.org/10.1038/s41401-020-00537-9. Epub 2020 Oct 12.PMID: 33041326; PMCID: PMC7548405.
[24] R.C. Hubrecht, E. Carter, The 3Rs and humane experimental technique: implementing change, Animals (2019) 754, https://doi.org/10.3390/ani9100754.
[25] R. Humeniuk, A. Mathias, H. Cao, A. Osinusi, G. Shen, E. Chng, J. Ling, A. Vu, P. German, Safety, tolerability, and pharmacokinetics of remdesivir, an antiviral for treatment of COVID-19, in healthy subjects, Clin. Transl. Sci. 13 (5) (2020) 896–906, https://doi.org/10.1111/cts.12840. Epub 2020 Aug 5. PMID: 32589775; PMCID: PMC7361781.
[26] C.M. Jacobsen, N. Narita, M. Bielinska, A.J. Syder, J.I. Gordon, D.B. Wilson, Genetic mosaic analysis reveals that GATA-4 is required for proper differentiation of mouse gastric epithelium, Jan 1, Dev. Biol. 241 (1) (2002) 34–46, https://doi.org/10.1006/dbio.2001.0424.
[27] S.C.J. Jorgensen, R. Kebriaei, L.D. Dresser, Remdesivir: review of pharmacology, pre-clinical data, and emerging clinical experience for COVID-19, Pharmacotherapy 40 (7) (2020) 659–671, https://doi.org/10.1002/phar.2429. Epub 2020 Jun 28. PMID: 32446287; PMCID: PMC7283864.
[28] S.C.J. Jorgensen, M.R. Davis, S.E. Lapinsky, A review of remdesivir for COVID-19 in pregnancy and lactation, J. Antimicrob. Chemother. 77 (1) (2021) 24–30, https://doi.org/10.1093/jac/dkab311. PMID: 34427297; PMCID: PMC8499800.
[29] H. Kagawa, A. Javali, H.H. Khoei, T.M. Sommer, G. Sestini, M. Novatchkova, Y. Scholte Op Reimer, G. Castel, A. Bruneau, N. Maenhoudt, J. Lammers, S. Loubersac, T. Freour, H. Vankelecom, L. David, N. Rivron, Human blastoids model blastocyst development and implantation, Dec 2, Nature 601 (2021) 600–605, https://doi.org/10.1038/s41586-021-04267-8.
[30] G. Kokic, H.S. Hillen, D. Tegunov, C. Dienemann, F. Seitz, J. Schmitzova, L. Farnung, A. Siewert, C. Höbartner, P. Cramer, Mechanism of SARS-CoV-2 polymerase stalling by remdesivir, Nat. Commun. 12 (1) (2021) 279, https://doi.org/10.1038/s41467-020-20542-0. PMID: 33436624; PMCID: PMC7804290.
[31] M. Kwok, C. Lee, H.S. Li, R. Deng, C. Tsoi, Q. Ding, S.Y. Tsang, K.T. Leung, B. P. Yan, E.N. Poon, Remdesivir induces persistent mitochondrial and structural damage in human induced pluripotent stem cell derived cardiomyocytes, Cardiovasc Res. (2021), cvab311, https://doi.org/10.1093/cvr/cvab311. Epub ahead of print. PMID: 34609482; PMCID: PMC8500104.
[32] A.M. Laeno, D.A. Tamashiro, V.B. Alarcon, Rho-associated kinase activity is required for proper morphogenesis of the inner cell mass in the mouse blastocyst, Biol. Reprod. 89 (5) (2013) 122, https://doi.org/10.1095/biolreprod.113.109470. PMID: 23946538; PMCID: PMC4434990.
[33] S. Lamas, J. Carvalheira, F. Gartner, I. Amorim, C57BL/6J mouse superovulation: schedule and age optimization to increase oocyte yield and reduce animal use, Zygote 29 (3) (2021) 199–203, https://doi.org/10.1017/S0967199420000714. Epub 2021 Jan 15.PMID: 33448261.
[34] R. Li, A. Liclican, Y. Xu, J. Pitts, C. Niu, J. Zhang, C. Kim, X. Zhao, D. Soohoo, D. Babusis, Q. Yue, B. Ma, B.P. Murray, R. Subramanian, X. Xie, J. Zou, J.P. Bilello, L. Li, B.E. Schultz, R. Sakowicz, B.J. Smith, P.Y. Shi, E. Murakami, J.Y. Feng, Key metabolic enzymes involved in remdesivir activation in human lung cells, Antimicrob. Agents Chemother. 65 (9) (2021), e0060221, https://doi.org/10.1128/AAC.00602-21. Epub 2021 Aug 17. PMID: 34125594; PMCID: PMC8370248.
[35] H.X.J. Lin, S. Cho, V. Meyyur Aravamudan, H.Y. Sanda, R. Palraj, J.S. Molton, I. Venkatachalam, Remdesivir in Coronavirus Disease 2019 (COVID-19) treatment: a review of evidence, Infection 49 (3) (2021) 401–410, https://doi.org/10.1007/s15010-020-01557-7. Epub 2021 Jan 2. PMID: 33389708; PMCID: PMC7778417.
[36] Y. Marikawa, V.B. Alarcon, Creation of trophectoderm, the first epithelium, in mouse preimplantation development, Results Probl. Cell Differ. 55 (2012) 165–184, https://doi.org/10.1007/978-3-642-30406-4_9. PMID: 22918806; PMCID: PMC3642205.
[37] Y. Marikawa, V.B. Alarcon, RHOA activity in expanding blastocysts is essential to regulate HIPPO-YAP signaling and to maintain the trophectoderm-specific gene expression program in a ROCK/actin filament-independent manner, Mol. Hum. Reprod. 25 (2) (2019) 43–60, https://doi.org/10.1093/molehr/gay048. PMID: 30395288; PMCID: PMC6497036.
[38] Y. Marikawa, H.R. Chen, M. Menor, Y. Deng, V.B. Alarcon, Exposure-based assessment of chemical teratogenicity using morphogenetic aggregates of human embryonic stem cells, Reprod. Toxicol. 91 (2020) 74–91, https://doi.org/10.1016/j.reprotox.2019.10.004. Epub 2019 Nov 8. PMID: 31711903; PMCID: PMC6980740.
[39] Y. Marikawa, M. Menor, Y. Deng, V.B. Alarcon, Regulation of endoplasmic reticulum stress and trophectoderm lineage specification by the mevalonate pathway in the mouse preimplantation embryo, Mol. Hum. Reprod. 27 (4) (2021), gaab015, https://doi.org/10.1093/molehr/gaab015. PMID: 33677573; PMCID: PMC7990410.
[40] S. Menchero, T. Rayon, M.J. Andreu, M. Manzanares, Signaling pathways in mammalian preimplantation development: linking cellular phenotypes to lineage decisions, Dev. Dyn. 246 (4) (2017) 245–261, https://doi.org/10.1002/dvdy.24471. Epub 2016 Dec 29. PMID: 27859869.
[41] K. Mitsui, Y. Tokuzawa, H. Itoh, K. Segawa, M. Murakami, K. Takahashi, M. Maruyama, M. Maeda, S. Yamanaka, The homeoprotein Nanog is required for maintenance of pluripotency in mouse epiblast and ES cells, Cell 113 (5) (2003) 631–642, https://doi.org/10.1016/s0092-8674(03)00393-3. PMID: 12787504.
[42] H. Mohammed, I. Hernando-Herraez, A. Savino, A. Scialdone, I. Macaulay, C. Mulas, T. Chandra, T. Voet, W. Dean, J. Nichols, J.C. Marioni, W. Reik, Single-cell landscape of transcriptional heterogeneity and cell fate decisions during mouse early gastrulation, Cell Rep. 20 (5) (2017) 1215–1228, https://doi.org/10.1016/j.celrep.2017.07.009. PMID: 28768204; PMCID: PMC5554778.
[43] M.A. Molè, A. Weberling, M. Zernicka-Goetz, Comparative analysis of human and mouse development: From zygote to pre-gastrulation, Curr. Top. Dev. Biol. 136 (2020) 113–138, https://doi.org/10.1016/bs.ctdb.2019.10.002. Epub 2019 Dec 26. PMID: 31959285.
[44] National Research Council (US) Committee for the Update of the Guide for the Care and Use of Laboratory Animals. Guide for the Care and Use of Laboratory Animals. 8th edition. Washington (DC): National Academies Press (US); 2011. doi: ⟨10.17226/12910⟩.

[45] J. Nichols, B. Zevnik, K. Anastassiadis, H. Niwa, D. Klewe-Nebenius, I. Chambers, H. Schöler, A. Smith, Formation of pluripotent stem cells in the mammalian embryo depends on the POU transcription factor Oct4, Cell 95 (3) (1998) 379–391, https://doi.org/10.1016/s0092-8674(00)81769-9. PMID: 9814708.
[46] P. Pagliano, C. Sellitto, G. Scarpati, T. Ascione, V. Conti, G. Franci, O. Piazza, A. Filippelli, An overview of the preclinical discovery and development of remdesivir for the treatment of coronavirus disease 2019 (COVID-19), Expert Opin. Drug Discov. 17 (1) (2022) 9–18, https://doi.org/10.1080/17460441.2021.1970743. Epub 2021 Aug 27. PMID: 34412564; PMCID: PMC8425432.
[47] B. Plusa, A. Piliszek, Common principles of early mammalian embryo self-organisation, Jul 22, Development 147 (14) (2020), dev183079, https://doi.org/10.1242/dev.183079.
[48] B. Plusa, A. Piliszek, S. Frankenberg, J. Artus, A.K. Hadjantonakis, Distinct sequential cell behaviours direct primitive endoderm formation in the mouse blastocyst, Development 135 (18) (2008) 3081–3091, https://doi.org/10.1242/dev.021519. PMID: 18725515; PMCID: PMC2768606.
[49] E. Posfai, S. Petropoulos, F.R.O. de Barros, J.P. Schell, I. Jurisica, R. Sandberg, F. Lanner, J. Rossant, Position- and Hippo signaling-dependent plasticity during lineage segregation in the early mouse embryo, Feb 22, Elife 6 (2017), e22906, https://doi.org/10.7554/eLife.22906.
[50] J. Rossant, Genetic control of early cell lineages in the mammalian embryo, Nov 23, Annu. Rev. Genet. 52 (2018) 185–201, https://doi.org/10.1146/annurev-genet-120116-024544.
[51] A.P. Russ, S. Wattler, W.H. Colledge, S.A. Aparicio, M.B. Carlton, J.J. Pearce, S. C. Barton, M.A. Surani, K. Ryan, M.C. Nehls, V. Wilson, M.J. Evans, Eomesodermin is required for mouse trophoblast development and mesoderm formation, Mar 2, Nature 404 (6773) (2000) 95–99, https://doi.org/10.1038/35003601.
[52] S.A. Saghir, M.A. Dorato, Reproductive and developmental toxicity testing: examination of the extended one-generation reproductive toxicity study guideline (Aug), Regul. Toxicol. Pharmacol. 79 (2016) 110–117, https://doi.org/10.1016/j.yrtph.2016.03.023.
[53] H. Sasaki, Roles and regulations of Hippo signaling during preimplantation mouse development (Jan), Dev. Growth Differ. 59 (1) (2017) 12–20, https://doi.org/10.1111/dgd.12335.
[54] B. Sozen, V. Jorgensen, B.A.T. Weatherbee, S. Chen, M. Zhu, M. Zernicka-Goetz, Reconstructing aspects of human embryogenesis with pluripotent stem cells, Nat. Commun. 12 (1) (2021) 5550, https://doi.org/10.1038/s41467-021-25853-4. PMID: 34548496; PMCID: PMC8455697.
[55] D. Strumpf, C.A. Mao, Y. Yamanaka, A. Ralston, K. Chawengsaksophak, F. Beck, J. Rossant, Cdx2 is required for correct cell fate specification and differentiation of trophectoderm in the mouse blastocyst, Development 132 (9) (2005) 2093–2102, https://doi.org/10.1242/dev.01801. Epub 2005 Mar 23.PMID: 15788452.
[56] M.C. Summers, A brief history of the development of the KSOM family of media, J. Assist. Reprod. Genet. 30 (8) (2013) 995–999, https://doi.org/10.1007/s10815-013-0097-8. PMID: 24046024; PMCID: PMC3790120.
[57] M. Tempestilli, P. Caputi, V. Avataneo, S. Notari, O. Forini, L. Scorzolini, L. Marchioni, T. Ascoli Bartoli, C. Castilletti, E. Lalle, M.R. Capobianchi, E. Nicastri, A. D'Avolio, G. Ippolito, C. Agrati, COVID 19 INMI Study Group. Pharmacokinetics of remdesivir and GS-441524 in two critically ill patients who recovered from COVID-19, J. Antimicrob. Chemother. 75 (10) (2020) 2977–2980, https://doi.org/10.1093/jac/dkaa239. PMID: 32607555; PMCID: PMC7337789.
[58] Y. Wang, L. Chen, Tissue distributions of antiviral drugs affect their capabilities of reducing viral loads in COVID-19 treatment, Eur. J. Pharmacol. 889 (2020), 173634, https://doi.org/10.1016/j.ejphar.2020.173634. Epub 2020 Oct 6.PMID: 33031797; PMCID: PMC7536545.
[59] E. Wicklow, S. Blij, T. Frum, Y. Hirate, R.A. Lang, H. Sasaki, A. Ralston, HIPPO pathway members restrict SOX2 to the inner cell mass where it promotes ICM fates in the mouse blastocyst, PLoS Genet. 10 (10) (2014), e1004618, https://doi.org/10.1371/journal.pgen.1004618. PMID: 25340657; PMCID: PMC4207610.
[60] Y. Xu, O. Barauskas, C. Kim, D. Babusis, E. Murakami, D. Kornyeyev, G. Lee, G. Stepan, M. Perron, R. Bannister, B.E. Schultz, R. Sakowicz, D. Porter, T. Cihlar, J.Y. Feng, Off-target in vitro profiling demonstrates that remdesivir is a highly selective antiviral agent, Antimicrob. Agents Chemother. 65 (2) (2021), https://doi.org/10.1128/AAC.02237-20. PMID: 33229429; PMCID: PMC7849018.
[61] L. Yan, M. Yang, H. Guo, L. Yang, J. Wu, R. Li, P. Liu, Y. Lian, X. Zheng, J. Yan, J. Huang, M. Li, X. Wu, L. Wen, K. Lao, R. Li, J. Qiao, F. Tang, Single-cell RNA-Seq profiling of human preimplantation embryos and embryonic stem cells (Sep), Nat. Struct. Mol. Biol. 20 (9) (2013) 1131–1139, https://doi.org/10.1038/nsmb.2660.
[62] A. Yanagida, D. Spindlow, J. Nichols, A. Dattani, A. Smith, G. Guo, Naive stem cell blastocyst model captures human embryo lineage segregation, Cell Stem Cell 28 (6) (2021) 1016–1022.e4, https://doi.org/10.1016/j.stem.2021.04.031. Epub 2021 May 5. PMID: 33957081; PMCID: PMC8189436.
[63] L. Yu, Y. Wei, J. Duan, D.A. Schmitz, M. Sakurai, L. Wang, K. Wang, S. Zhao, G. C. Hon, J. Wu, Blastocyst-like structures generated from human pluripotent stem cells, Nature 591 (7851) (2021) 620–626, https://doi.org/10.1038/s41586-021-03356-y. Epub 2021 Mar 17. Erratum in: Nature. 2021 Aug;596(7872):E5. PMID: 33731924.
[64] C. Zhang, C. Liu, D. Li, N. Yao, X. Yuan, A. Yu, C. Lu, X. Ma, Intracellular redox imbalance and extracellular amino acid metabolic abnormality contribute to arsenic-induced developmental retardation in mouse preimplantation embryos, J. Cell Physiol. 222 (2) (2010) 444–455, https://doi.org/10.1002/jcp.21966.